Mechanical model for the tectonics of doubly vergent compressional orogens

Sean Willett
Christopher Beaumont
Philippe Fullsack
Department of Oceanography, Dalhousie University, Halifax, Nova Scotia B3H 4J1, Canada

ABSTRACT

A mechanical model of crustal shortening and deformation driven by the relative convergence of rigid, underlying mantle plates explains many features of convergent orogens. Results based on numerical models and supported by sandbox models show that a Coulomb crustal layer subject to basal velocity boundary conditions corresponding to asymmetric detachment and subduction of the underlying mantle passes through three stages of orogenic growth: (1) block uplift bounded by step-up shear zones; (2) development of a low-taper wedge over the underthrusting mantle plate; and (3) development of a low-taper wedge overlying the overthrusting mantle plate and verging in the opposite direction. When modified by isostasy, basal viscous flow, surface erosion and denudation, and sedimentation, the resultant model orogens exhibit a variety of styles with characteristics in common with small, rapidly denuded orogens, large orogens with plateaus and extensional characteristics, and active subduction margins with doubly vergent accretionary wedges and deformed fore-arc basins.

INTRODUCTION

The doubly vergent nature of continental collision zones was noted early in this century (Argand, 1916) and more recently for active margins (e.g., Silver and Reed, 1988; Byrne et al., 1988) (Fig. 1, A and B). Investigation of the underlying mechanics has, however, been confined mainly to sandbox experiments (Malavieille, 1984). Critical Coulomb wedge models (e.g., Davis et al., 1983; Dahlen, 1984, 1990) can explain the geometry of accretionary wedges but are limited in their applicability to the structure of the orogen as a whole. We present results from a mechanical model, based on more general numerical techniques, in which a crustal layer with a rigid-plastic rheology is deformed by the motion of two nearly rigid, underlying plates. Calculations were made with a velocity-based, Eulerian, finite-element technique (Willett, 1992; Beaumont et al., 1992a), but results presented here are restricted to interpretive descriptions.

BASIC MODEL: DOUBLY VERGENT CRITICAL MECHANICS

Description of Basic Model

We consider first the two-dimensional, plane-strain deformation of a laterally uniform, rigid-plastic layer attached to two converging, rigid underlying plates. One underlying plate is assumed to slide below the other at point S, and their motion imposes constant-velocity boundary conditions on the base of the overlying layer (Fig. 1C). Left of S the velocity is constant and positive (moving from left to right), whereas to the right of S it is zero (Fig. 1C). The discontinuity in the horizontal boundary velocity at S results in a singularity in the strain rate field within the layer. The model layer is infinite in lateral extent (X direction, Fig. 1C). These boundary conditions are fundamentally asymmetric, as illustrated by the model results.

The deforming layer has a noncohesive Coulomb yield criterion with a coefficient of friction ϕ. The base of the layer is weaker than the overlying material and has a coefficient of friction ϕ_b. The flow rule that governs the post-yield deformation is isotropic and incompressible, and the material does not strain harden or soften. With these properties and boundary conditions, the problem is scale independent and so is applicable for any layer thickness H.

Results of the Basic Model

Initially, the basic model shows two conjugate zones of shear deformation that "step up" deformation from the stress singularity to the surface (Fig. 1C). Consistent with the incompressible Coulomb plastic rheology, the shear zones initially form at 45° relative to the direction of maximum compressive stress, which is approximately horizontal. The initial stress and strain rate fields are symmetric, but subsequent growth is distinctly asymmetric and remains so through three stages of development (Fig. 2).

In stage 1 (Fig. 2A), the step-up shear zones remain rooted at the singularity. The region between the shear zones forms a nearly undeforming triangular plug that is lifted and translated to the right to form a block uplift.

In stage 2 (Fig. 2B), deformation propagates beyond the step-up

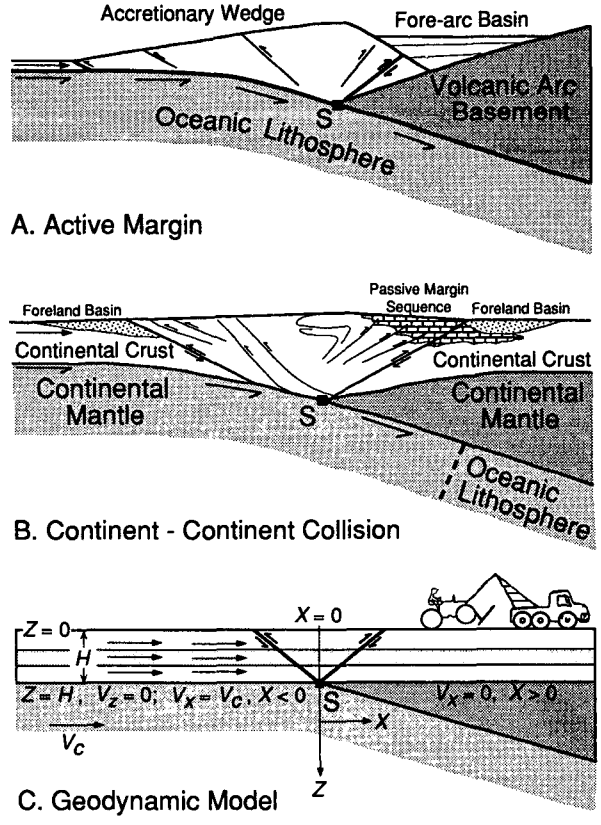

Figure 1. Illustration of active margin (A) and continent-continent collision (B). Crustal deformation is focused above point S, where mantle of left plate detaches and is underthrust. C: Geodynamic model in which uniform crust, extending from surface to depth H, is deformed under basal velocity boundary conditions. Underlying domain (gray regions) is not modeled. For these boundary conditions there is no requirement for "bulldozer" backstop.

shear zones as the layer begins to shear on detachments that develop on the base between the singularity and the deformation front. Basal detachment occurs first to the left, or upstream, of the singularity. We call this the "pro" direction and the overlying zone of deformation the pro-wedge. Downstream of the singularity is termed the "retro" direction and its zone of deformation is called the retro-wedge (Fig. 2B). During stage 3 (Fig. 2C), the retro-wedge detaches from its base, and the deformation front propagates significantly into the undeformed layer to the right and initiates the formation of a lower taper wedge.

Deformation is similarly asymmetric, the pro-wedge strain being more diffuse than strain in the retro-wedge. This is the result of the movement of material through the pro-wedge. In contrast, material deformed in the retro-wedge remains in place and undergoes more concentrated deformation.

Comparison with Sandbox Models

The basic model can be compared with equivalent sandbox experiments. Although both materials have Coulomb yield properties, there are two differences. First, sand shows strain localization on numerous small-scale faultlike structures, in contrast with the distributed continuum deformation of our numerically based models. Second, unlike the incompressible numerical model, sand dilates on initial deformation so that failure occurs according to Coulomb theory at angles of $\pm[45-(\phi/2)]$ to the principal axes. Therefore sandbox faults dip at lower angles than the shear zones in the numerical model. The numerical model corresponds to a high-pressure sandbox experiment (Hobbs et al., 1990).

Despite these differences, sandbox experiments with the same boundary conditions exhibit the same initial failure and subsequent asymmetric development of pro- and retro-wedges as the basic model. Malavieille (1984) showed experimental results equivalent to stages 1 and 2 (Fig. 2). Wang and Davis (1992) extended the experiment to stage 3 showing the same kinked retro-wedge surface slope as the basic model. Experiments by Byrne et al. (1988, 1993) and Koons (1990) have somewhat different boundary conditions, but similar results.

Comparison with Uniform-Taper Critical Coulomb Wedges

Some aspects of our basic model can be understood through critical Coulomb wedge theory (e.g., Davis et al., 1983; Dahlen, 1984, 1990). Deformation in stage 1 is dominated by the finite thickness of the layer, but with increased convergence, the parts of the pro- and retro-wedges removed from the toe or the singularity develop with a uniform taper, as predicted by Coulomb wedge theory (Fig. 2B). The pro-wedge has the geometry and stress solution corresponding to the *minimum* taper angle predicted by critical Coulomb wedge theory. The retro-wedge, in contrast, is steeper and corresponds to the *maximum* permissible taper angle (Dahlen, 1984). This different mechanical behavior is the response to the kinematics of growth; a wedge grown from accretion at the toe (as in the case of the pro-wedge) has the minimum taper angle, and a wedge grown from material added at the back and transported across the singularity (retro-wedge) has the maximum taper angle.

At the third and largest stage of growth (Fig. 2C) the retro-wedge shows a break in slope. This slope break represents a spatial transition from the maximum taper to a minimum taper, as material is accreted to the toe of the retro-wedge.

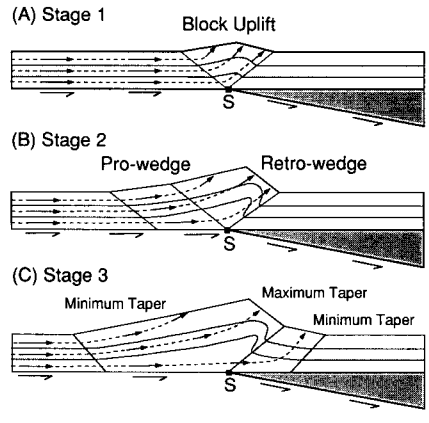

Figure 2. Stages of basic model development. Shaded layer is passive marker. Dashed lines are instantaneous flow lines, not particle trajectories. Arrows are proportional to velocity.

GEOLOGIC PROCESSES MODIFYING THE BASIC MODEL

The basic model illustrates the mechanics of the simplest case of asymmetric, doubly vergent tectonics, but if it is to be applied to natural orogens (Fig. 1, A and B), other processes must be incorporated.

Isostasy

Isostatic compensation profoundly affects the cross-section shape and mass balance of a growing, crustal-scale orogen and requires more crustal rock to be assimilated into the orogen to achieve the same development (Fig. 3A). Surface slopes are also modified by the changing shape of the base. A crustal root develops with either local or regional (flexural) compensation models. With flexural compensation, the undeformed plate on either side is flexed downward adjacent to the orogenic belt, resulting in a foredeep and the formation of a foreland basin (Fig. 3A). Negative buoyancy of the subducted lower lithosphere may further enhance this effect.

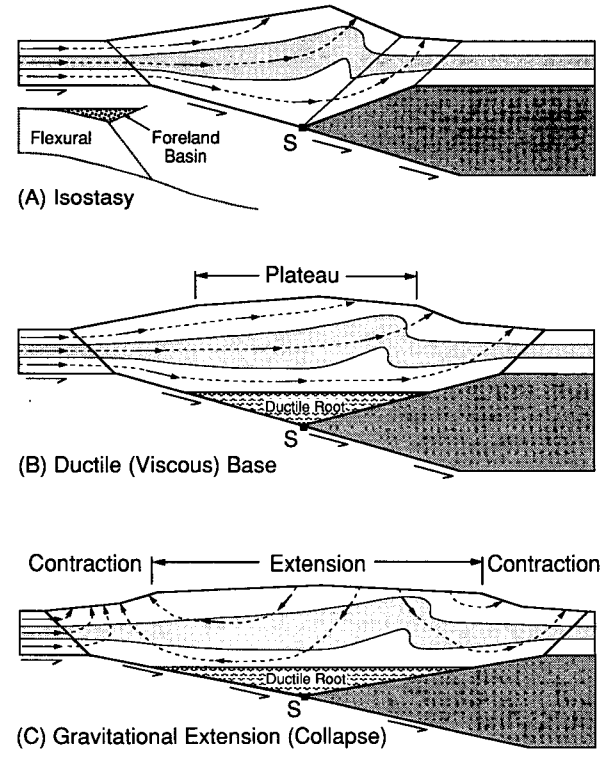

Figure 3. Effects of isostasy and viscous (ductile) flow in lower crust (Fig. 2C). A: Isostasy, stylized local and flexural. B: Decrease in basal shear strength as temperature increases creates plateau bounded by frictional-based pro- and retro-wedges. C: Further increase in lower crustal temperature or decrease in convergence rate makes interior plateau extend and increases contraction in frictional-based bounding wedges. Dashed lines are instantaneous flow lines, not particle trajectories. Arrows are proportional to velocity.

Thermally Activated Viscous Lower Crust

As an orogen continues to grow and the crust thickens, the lower crust increases in temperature as a result of the increased depth of burial. Eventually, this increase in temperature results in a change in the dominant deformational mechanism from a frictional, Coulomb plasticity to thermally activated, nonlinear viscous flow (loosely termed the brittle-ductile transition). Viscous flow in the lower crust implies a weak base to the orogen, resulting in a low surface slope. As a consequence, a low-angle plateau forms over the interior of the orogen (Fig. 3B).

As the viscous base of an orogen becomes progressively hotter and weaker, the taper angle must decrease, and the orogen deforms to accommodate this requirement. However, if the rate of heating is too high for accretionary deformation to adjust the taper accordingly, the internal region of the orogen enters a state of extension, collapsing and thereby achieving the required taper angle (Fig. 3C). The external regions of the orogen are still controlled by a frictional Coulomb rheology and remain in horizontal contraction as deformation drives material outward by extension of the orogen interior. The occurrence of simultaneous orogenic extension and contraction is therefore a predicted consequence of basal weakening.

The strain rate dependence of viscous shear stresses also implies that the geometry (taper angle) of a viscous-based orogen depends on the convergence velocity. A change in convergence velocity, therefore, implies a change in orogen geometry. A large decrease in convergence velocity can require the orogen to enter a state of horizontal extension to achieve a new, stable geometry (Fig. 3C). In particular, if convergence stops, the interior of a viscous-based orogen *must* extend until no surface slope remains across the interior plateau.

Surface Erosion and Denudation

The critical, at-yield mechanical state of the material in a deforming orogen implies a strong interdependence between the active deformation of the orogen and its topographic profile. Surface processes that erode and denude mountains lead to large-scale removal of mass from an orogen and cause the velocity field to adjust to replace eroded material by material from within. The at-yield behavior of the model orogen requires that deformation adjust instantaneously to replace removed material. Denuded zones therefore have enhanced exhumation rates.

The importance of this mass replacement feedback on exhumation rates is best appreciated by considering the steady-state behavior of small collisional orogens undergoing asymmetrical denudation. This situation occurs where precipitation is orographically controlled, giving the orogen a wet, rapidly denuded, windward side and a dry side with little erosional denudation. Steady-state retro-wedge denudation (Fig. 4A) modifies rock trajectories to exhume highest grade metamorphic rocks at the retro-deformation front, which is dynamically pinned by windward denudation. The replacement mass is derived from the pro-wedge; therefore, the pressure-temperature history of material in the orogen must reflect the path and time taken for mass to move across the entire width of the orogen. There is no net growth, uplift, or exhumation of the pro-wedge. The central Southern Alps orogen of New Zealand appears to have this style (Norris et al., 1990). The retro-wedge faces windward to the Tasman Sea, and the step-up shear zone on the retro-side is the Alpine fault. The surface metamorphic-grade distribution, cooling histories of exhumed rocks, and rock affinities agree with model predictions (Fig. 4A). In this situation, the highest grade rocks are exhumed near the toe of the orogen at low elevation, not in the high interior.

In contrast, steady-state pro-wedge denudation creates a non-deforming, noneroding retro-wedge against which pro-wedge material is decoupled and exhumed (Fig. 4B). This response has the effect of short-circuiting the material trajectories and subsequently reducing the path length and residence time in the orogen. Under steady-state pro-wedge denudation, the metamorphic grade of surface rocks increases across the pro-wedge (Fig. 4B), closely paralleling Barr and Dahlen's (1991) analysis of Taiwan, and the highest grade rocks are exhumed in the orogen interior at high elevation against the nondeforming retro-wedge. Note that the retro-wedge is nondeforming only when the orogen is in a steady or destructive state as defined by Jamieson and Beaumont (1989). Retro-wedge deformation will return as growth resumes.

Sedimentation at Active Margins

Sedimentation over actively deforming regions of an orogen acts to reduce the surface slope, thereby bringing the stress state of the orogenic wedge below critical. The wedge must deform to steepen the slope and bring the wedge back to critical before the deformation front can propagate.

This interaction between deformation and sedimentation is particularly well illustrated at active margins, where fore-arc sedimentation occurs over the actively accreting wedge. Apart from sedimentation and the development of a fore-arc basin, active margins show many of the characteristics of the doubly vergent tectonic model, i.e., a large accretionary wedge obeying pro-wedge mechanics and a smaller landward-verging retro-wedge, landward of an outer-arc high and overlying the arc basement (Byrne et al., 1988) (Fig. 1A). The disparity in size between the two wedges is largely the result of fore-arc sedimentation. As the doubly vergent wedge grows, sediments are ponded between the volcanic arc and the outer-arc

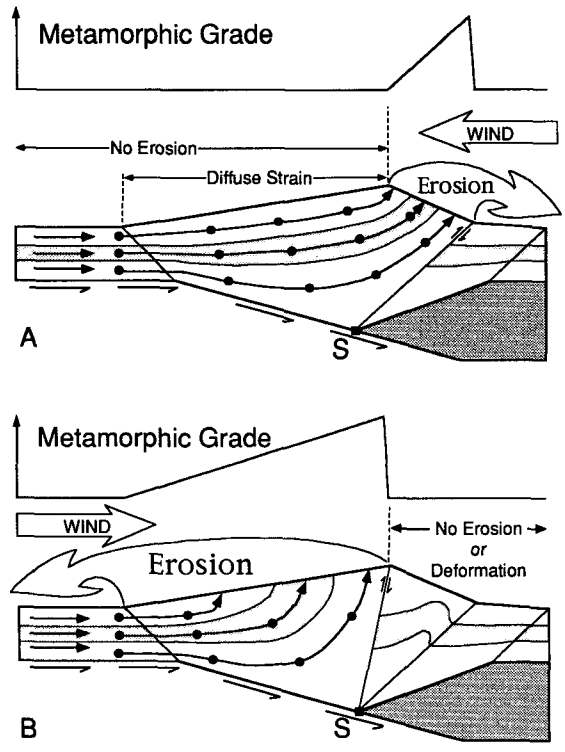

Figure 4. Effect of steady-state (constant geometry and mass) erosion and denudation. A: Retro-wedge denudation. B: Pro-wedge denudation. Passive shaded layer shows exhumed position of middle crust. Lines are material trajectories; dots are progressive equal-time positions of points initially aligned vertically. Schematic metamorphic grade is for surface rocks assuming initial equilibrium conditions.

high that overlies the singularity; these sediments cover the retro-wedge, reduce its surface slope, and thus inhibit its landward growth. In order to balance the growth of the pro-wedge, the back of the retro-wedge deforms and uplifts along a zone of shear propagating from the singularity (Fig. 5). The Barbados Ridge is a good example of this style of deformation (Westbrook et al., 1988).

The landward growth of the retro-wedge and the formation of a fore-arc basin are coupled through the balance between growth of the orogenic wedges and sedimentation in the fore arc. While sediment fills the depression between the arc and the outer-arc high, the retro-wedge cannot grow and deformation remains localized on the arc side of the outer-arc high (Fig. 5). However, if accretion rates are sufficiently high that the outer-arc high grows a landward-dipping topographic slope, the retro-wedge will propagate landward, progressively deforming the fore-arc basin. When sedimentation rates and accretion rates change over geologic time, fore-arc basin stratigraphy and deformational history reflect intervals when the wedge propagated into the fore-arc basin and times when increased sedimentation suppressed deformation.

DISCUSSION AND CONCLUSIONS

The numerical models presented in this paper, and confirmed in the basic example by sandbox experiments, demonstrate the fundamentally asymmetric mechanics of doubly vergent orogens, the asymmetry being related to the sense of subduction. The models reproduce successfully some of the wide range of deformational behavior of modern and ancient orogens within the framework of doubly vergent wedge mechanics.

The basic model results are the most simple style of crustal deformation to be expected in an accretionary or collisional orogen where (1) the deforming crustal layer is an incompressible Coulomb plastic layer with a weaker base, (2) the properties of the crustal layer have no significant lateral variations, (3) the convergence direction is normal to the orogen, and (4) convergence is fundamentally controlled by the detachment and underthrusting of the lithosphere by one of the plates in a subductionlike manner.

The basic model only provides a guide to geologic applications. Modifications and alterations to the model as consequences of isostasy, Coulomb plastic to viscous (brittle to ductile) transition in the lower crust, and surface denudation and deposition have been noted.

We caution that the investigation is incomplete. There are additional factors that have profound effects on the model orogens and remain to be examined in detail. For example, rheological layering of the model crust permits intracrustal detachment and deformation styles that mimic the behavior of thin-skinned and thick-skinned thrust and fold belts (Beaumont et al., 1992b).

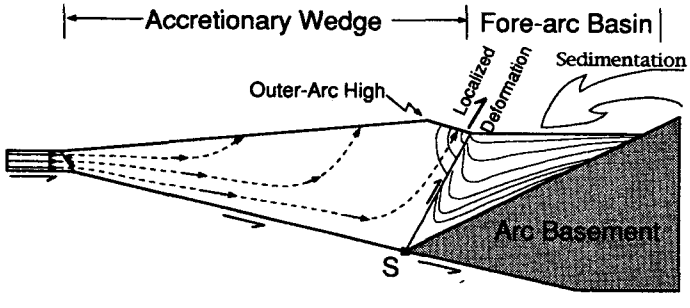

Figure 5. Effect of fore-arc sedimentation, ponded between volcanic arc and outer-arc high and overlying retro-wedge, in inhibiting arcward growth of retro-wedge. Deformation is limited to edge of fore-arc basin but would propagate into basin were sedimentation rates to decline. Dashed lines are instantaneous flow lines, not particle trajectories.

The analysis has also been limited to consideration of only one set of velocity boundary conditions (Fig. 1C). The more general problem includes positive or negative velocities on either side of the basal boundary with respect to the singularity (Fig. 1C), reproducing tectonic settings that include retreat (rollback) and advance of the subducting layer, double subduction, and net extension. In some tectonic settings there may be more than one basal velocity discontinuity and associated stress singularity.

The doubly vergent wedge model provides a useful and general framework for interpretation of the large-scale structure and mechanical behavior of convergent orogens.

ACKNOWLEDGMENTS

Funded by Natural Science and Engineering Research Council Operating, Lithoprobe, and Strategic grants to Beaumont. Willett was supported by I. W. Killam and Natural Science and Engineering Research Council International Fellowships. Leigh Royden and Raymond Fletcher provided helpful reviews of the manuscript. Becky Jamieson, Glen Stockmal, and Peter Koons commented on an earlier version. Lithoprobe Contribution No. 420.

REFERENCES CITED

Argand, E., 1916, Sur l'arc des Alpes occidentales: Ecologae Geologicae Helvetiae, v. 14, p. 145–191.

Barr, T.D., and Dahlen, F.A., 1991, Brittle frictional mountain building. 3. Low grade metamorphism: Journal of Geophysical Research, v. 96, p. 10,319–10,338.

Beaumont, C., Fullsack, P., and Hamilton, J., 1992a, Erosional control of active compressional orogens, *in* McClay, K.R., ed., Thrust tectonics: London, Chapman and Hall, p. 1–18.

Beaumont, C., Fullsack, P., Hamilton, J., and Willett, S., 1992b, Preliminary results from a mechanical model of the tectonics of compressive crustal deformation, *in* Ross, G.M., ed., Alberta basement transects, workshop report, Volume 28: Lithoprobe Secretariat, University of British Columbia, p. 22–61.

Byrne, D.E., Davis, D.M., and Sykes, L.R., 1988, Loci and maximum size of thrust earthquakes and the mechanics of the shallow region of subduction zones: Tectonics, v. 7, p. 833–857.

Byrne, D.E., Wang, W., and Davis, D.M., 1993, Mechanical role of backstops in the growth of fore arcs: Tectonics (in press).

Dahlen, F.A., 1984, Noncohesive critical Coulomb wedges: An exact solution: Journal of Geophysical Research, v. 89, p. 10,125–10,133.

Dahlen, F.A., 1990, Critical taper model of fold-and-thrust belts and accretionary wedges: Annual Review of Earth and Planetary Sciences, v. 18, p. 55–99.

Davis, D., Suppe, J., and Dahlen, F.A., 1983, Mechanics of fold-and-thrust belts and accretionary wedges: Journal of Geophysical Research, v. 88, p. 1153–1172.

Hobbs, B.E., Mühlhaus, H.-B., and Ord, A., 1990, Instability, softening and localization of deformation, *in* Knipe, R.J., and Rutter, E.H., eds., Deformation mechanisms, rheology and tectonics: Geological Society of London Special Publication 54, p. 143–165.

Jamieson, R.A., and Beaumont, C., 1989, Orogeny and metamorphism: A model for deformation and pressure-temperature-time paths with application to the central and southern Appalachians: Tectonics, v. 7, p. 417–445.

Koons, P.O., 1990, The two-sided orogen: Collision and erosion from the sandbox to the Southern Alps, New Zealand: Geology, v. 18, p. 679–682.

Malavieille, J., 1984, Modélisation expérimentale des chevauchements imbriqués: Application aux chaînes des montagnes: Société Géologique de France, Bulletin, v. 26, p. 129–138.

Norris, R.J., Koons, P.O., and Cooper, A.F., 1990, The obliquely-convergent plate boundary in the South Island of New Zealand: Implications for ancient collision zones: Journal of Structural Geology, v. 12, p. 715–725.

Silver, E.A., and Reed, D.L., 1988, Backthrusting in accretionary wedges: Journal of Geophysical Research, v. 93, p. 3116–3126.

Wang, W.H., and Davis, D.M., 1992, Sandbox model simulation of fore-arc evolution [abs.]: Eos (Transactions, American Geophysical Union), v. 73, p. 293.

Westbrook, G.K., Ladd, J.W., Buhl, P., Bangs, M., and Tiley, J.G., 1988, Cross section of an accretionary wedge: Barbados Ridge complex: Geology, v. 16, p. 631–635.

Willett, S., 1992, Dynamic and kinematic growth and change of a Coulomb wedge, *in* McClay, K.R., ed., Thrust tectonics: London, Chapman and Hall, p. 19–31.

Manuscript received July 10, 1992
Revised manuscript received December 14, 1992
Manuscript accepted December 29, 1992